Morphology and Field-Effect Mobility of Charge Carriers in Binary Blends of Poly(3-hexylthiophene) with Poly[2-methoxy-5-(2-ethylhexoxy)-1,4-phenylenevinylene] and Polystyrene

Amit Babel and Samson A. Jenekhe*

Department of Chemical Engineering and Department of Chemistry, University of Washington, Box 351750, Seattle, Washington 98195-1750

Received August 29, 2004; Revised Manuscript Received October 8, 2004

ABSTRACT: Two series of binary blends of regioregular poly(3-hexylthiophene) (PHT) with a polymer semiconductor, poly[2-methoxy-5-(2-ethylhexoxy)-1,4-phenylenevinylene] (MEH−PPV), and with an insulating polymer, polystyrene, were investigated and found to be phase separated and to exhibit relatively high field-effect mobility of holes ($(0.1-6) \times 10^{-3}$ cm^2/(V s)). Atomic force microscopy showed nucleation and growth type phase separation on the length scale of 100−600 nm in the binary blend systems. The mobility of holes in PHT/polystyrene blends is up to 7-fold higher than in PHT/MEH−PPV blends. The reduced carrier mobility in the PHT/MEH−PPV blends is due to dipolar effects arising from the polarity of the components. These results show for the first time that dipolar effects can substantially modify the charge transport properties of blends of conjugated polymers.

Introduction

Conjugated polymer semiconductors are of broad interest for diverse applications in organic electronics including light-emitting diodes for displays,[1−3] thin film transistors,[4,5] photovoltaic cells,[6] and electrochromic devices.[7] The synthesis of new conjugated polymers and copolymers represents one approach to tuning and optimizing the electronic and optoelectronic properties for these applications.[1−3] Blends represent an alternative means to the same end.[8−12] Compared to homopolymers, however, blends of conjugated polymers can exhibit novel properties such as photoinduced charge transfer,[8,9] exciplex formation,[9] efficient energy transfer,[10] exciton confinement,[11] and bipolar conductivity,[12] depending on the nature of the intermolecular interactions and features of the self-organization. We recently reported studies of the first thin film transistors based on blends of conjugated polymers.[13] Unusual blend composition dependence of the field-effect mobility of electrons[13a] and holes[13b,c] and relatively high hole mobilities were discovered. For a detailed understanding of charge transport in blends of polymer semiconductors to emerge, it is important to investigate other useful phase-separated polymer blend systems.

Poly[2-methoxy-5-(2-ethylhexoxy)-1,4-phenylenevinylene] (MEH−PPV) is an extensively studied electroluminescent polymer that finds applications in orange-red LEDs,[1,2,3f] photovoltaic diodes,[6a,d] and optically pumped lasers.[14] It has a rather low mobility of holes, $10^{-7}-10^{-6}$ cm^2/(V s), depending on the solvent from which films were cast, as determined from time-of-flight (TOF) measurements.[15] Although low carrier mobility is not a major problem in LEDs, it makes MEH−PPV not an important material for applications in thin film transistors. In contrast to MEH−PPV, solution cast films of regioregular poly(3-hexylthiophene) (PHT) have field-effect mobility of holes as high as 0.02−0.1 cm^2/(V s).[4,13b] PHT has thus far been the best polymer semiconductor for p-channel thin film transistors. Blends of MEH−PPV and PHT have been reported to have enhanced electroluminescence quantum efficiency.[16] Charge transport, particularly the field-effect mobility of charge carriers, in such PHT/MEH−PPV blends has not been reported. In general, knowledge of the field-effect charge carrier mobilities in blends of polymer semiconductors is of broad interest for improving and optimizing electronic and optoelectronic devices incorporating them.

In this paper, we report studies of a series of binary blends of MEH−PPV and PHT including the morphology and the charge carrier mobility. The compositional dependence of the charge carrier mobility in PHT/MEH−PPV blends was investigated by using thin film field-effect transistors (Figure 1). It has been shown in "molecularly doped" polymers, where hole-transport molecules such as triarylamines are dispersed in an insulating polymer, that the mobility of charge carriers is strongly dependent upon the host polymer.[17] Therefore, for comparison with the PHT/MEH−PPV blends, we have also investigated the morphology and the field-effect mobility of holes in a series of blends of PHT with polystyrene, an insulator and an *apolar* polymer. Atomic force microscopy (AFM) was used to investigate the blend morphology. The photophysical properties of the PHT/MEH−PPV blends were also investigated.

Experimental Section

Materials. The regioregular PHT sample with head-to-tail (HT) coupling exceeding 98.5% ($M_w \sim 19\,398$) was purchased from Aldrich. MEH−PPV ($M_w \sim 85\,000$) was obtained from American Dye Source, Inc., and the polystyrene ($M_w \sim 100\,000$) was from Polysciences, Inc. High-purity HPLC grade chloroform was used for making polymer solutions and the corresponding binary blends.

Two series of binary blends of PHT with MEH−PPV (10, 20, 30, 40, 50, 60, 70, 80, 90, and 100 wt % PHT) and with polystyrene (10, 20, 35, 50, 65, 80, and 90 wt % PHT) were prepared by mixing the appropriate volumes of 0.5 wt %

* Corresponding author: e-mail jenekhe@u.washington.edu.

10.1021/ma0482314 CCC: $27.50
Published on Web 11/25/2004

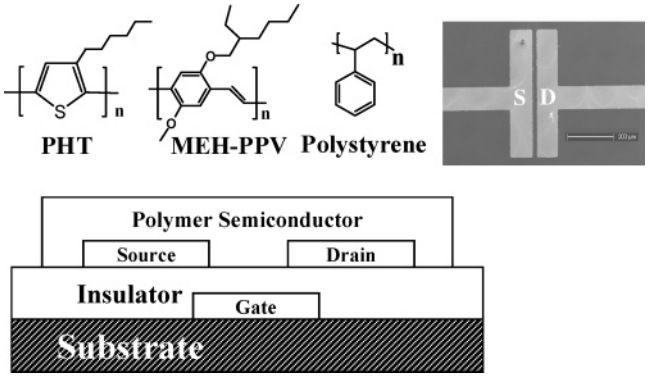

Figure 1. Molecular structures of binary blend components (PHT, MEH−PPV, and polystyrene) and a schematic of the thin film transistor. Inset shows an SEM image of the device.

solutions of the corresponding homopolymers in chloroform. Blend composition in this paper refers to weight percentage (or, weight fraction, x) of PHT, which is the common component in both blend systems. All thin films of the homopolymers and blends were spin-coated from chloroform solutions at a spin rate of 1200 rpm for 30 s. The films were dried overnight (10−12 h) at 60 °C in a vacuum oven to remove any residual solvent. Blend films (20−30 nm thick) spin-coated on glass slides for optical measurements were homogeneous and showed good optical transparency.

Atomic Force Microscopy of Polymer Thin Films. The thin film morphology of homopolymers and their blends was studied by using atomic force microscopy (AFM) (Digital Instruments, Santa Barbara, CA) in standard tapping mode. The thin films were spin-coated from their chloroform solutions onto a Si substrate with a 300 nm SiO_2 surface in order to emulate the field-effect transistor structure. The film thickness of the polymer samples used for AFM imaging was 20−30 nm. The film thickness was measured by an Alpha-Step 500 profilometer (KLA Tencor, Mountain View, CA) with an accuracy of 1 nm.

Optical Absorption and Photoluminescence Spectroscopy. Optical absorption spectra were obtained by using a Perkin-Elmer Lambda 900 UV/vis/near-IR spectrophotometer. Steady-state photoluminescence (PL) spectra were obtained on a Spex Fluorolog-2 spectrofluorimeter. The films were positioned such that the emitted light was detected at 22.5° from the incident beam. Further details of the photophysical characterization are similar to our previous reports.[3e,18]

Fabrication and Characterization of Thin Film Transistors. Bottom contact geometry was used to fabricate the thin film field-effect transistors as shown in Figure 1. Heavily doped Si with a conductivity of 10^3 S/cm was used as a gate electrode with 300 nm thick SiO_2 layer as the gate dielectric. Using photolithography and a vacuum sputtering system (2×10^{-6} Torr), two 90 nm thick gold electrodes (source and drain) with a 10 nm thick adhesive layer of TiW alloy were fabricated onto the SiO_2 layer. A channel length (L) of 25 μm and a channel width (W) of 500 μm were used. A gold contact pad was also deposited onto the gate electrode to make Ohmic contact. On top of this device structure thin films (20−30 nm) of PHT or MEH−PPV or a binary blend were spin-coated from chloroform solutions and dried overnight (10−12 h) at 60 °C in a vacuum oven. Electrical characteristics of these devices were measured using an HP 4155A semiconductor parameter analyzer (Yokogawa Hewlett-Packard, Tokyo). All the measurements were done under ambient laboratory conditions with reduced light exposure in the case of devices containing MEH−PPV.

Results and Discussion

Morphology of Binary Blends. Figure 2 shows the AFM topographic images of PHT/MEH−PPV blend thin films on Si/SiO_2 substrates as a function of composition. The AFM images of PHT homopolymer showed a

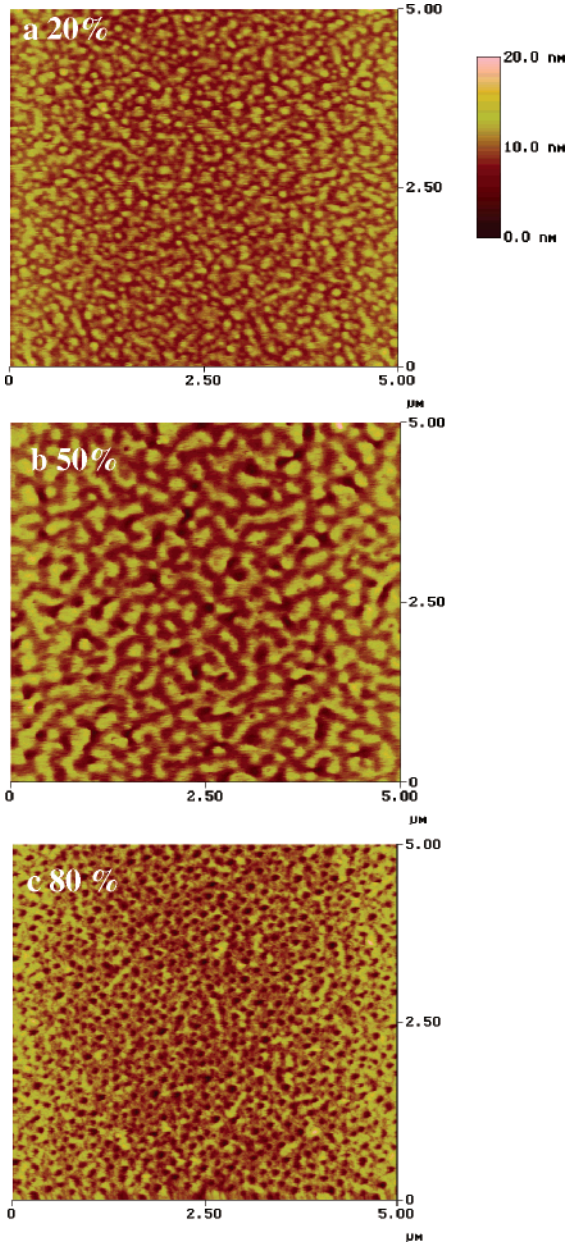

Figure 2. AFM topographic images of 20% (a), 50% (b), and 80% (c) PHT/MEH−PPV blend thin films on SiO_2 surface on a silicon substrate.

homogeneous surface morphology with some nanorod-like crystalline domain characteristic of the ordered regioregular PHT thin films.[13b] The AFM images of MEH−PPV homopolymer showed a smooth and featureless surface morphology. Two distinct phases can be seen in the AFM images of the blend thin films. The light features in Figure 2a−c increase with increasing PHT content in the blends, indicating that the light regions represent the PHT phase. The length scale of phase separation is about 100−200 nm. In blends containing 10−40 wt % PHT 100−200 nm in size, nearly spherical domains were observed. The domains increased in size with increasing composition of the minority phase (PHT), suggesting that the phase-separated morphology is of nucleation and growth type. In the 50 wt % PHT blend, a two-phase bicontinuous network was observed, and this indicates dimixing via spinodal decomposition (Figure 2b). Above 50% PHT, a reversal in surface morphology was observed with

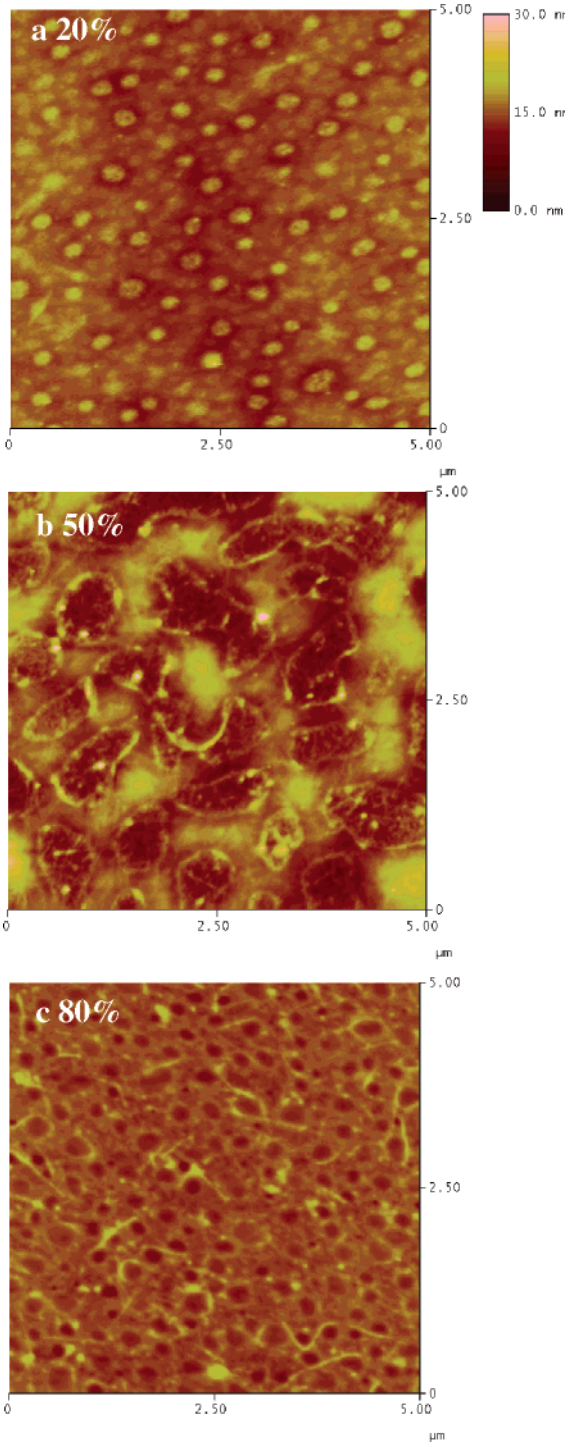

Figure 3. AFM topographic images of 20% (a), 50% (b), and 80% (c) PHT/polystyrene blend thin films on SiO_2 surface on a silicon substrate.

MEH−PPV phase (minor phase) forming the spherical domains. For example, in the 80 wt % PHT blend, the thin film morphology is shown in Figure 2c; the dark spherical domains are the MEH−PPV phase whereas the PHT phase (light region) shows a few rodlike domains characteristic of the PHT homopolymer. This indicates that some degree of ordering of the PHT phase exists in the blend thin films.

A similar phase-separated morphology was observed in PHT/polystyrene blends as shown in Figure 3a−c. The topographic AFM images of the 20 and 80 wt % PHT blends, where one of the phases is in the minority,

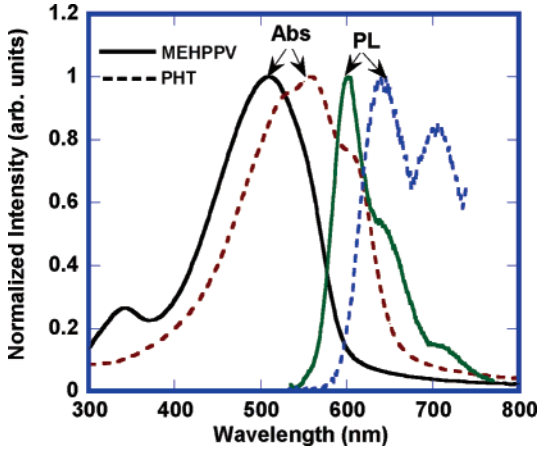

Figure 4. Normalized thin film optical absorption and PL emission spectra of PHT and MEH−PPV homopolymers.

show nucleation and growth type of phase-separation dynamics on the length scale of 400−600 nm (Figure 3a,c). In the symmetric blend composition (50 wt %), unlike the PHT/MEH−PPV blends, the PHT/polystyrene blend does not form a bicontinuous network. Instead, large isolated 1 μm islands of one of the phases can be seen (Figure 3b). In the 80 wt % blend (Figure 3c), where the majority phase is PHT, randomly oriented nanorodlike crystallites of PHT can be seen.

Photophysical Properties of PHT/MEH−PPV Blends. Optical absorption and photoluminescence (PL) spectra of thin films of PHT and MEH−PPV are shown in Figure 4. PHT has an absorption peak at 560 nm and an absorption band edge around 650 nm (1.9 eV). The PL emission spectrum of PHT (560 nm excitation) has a peak at 660 nm and a minor band at 720 nm. MEH−PPV has an absorption peak at 509 nm and an absorption band edge around 600 nm (2.1 eV). The PL emission spectrum of MEH−PPV (509 nm excitation) has an emission peak at 602 nm and a minor band around 650 nm. The PL spectrum of MEH−PPV and the absorption spectrum of PHT overlap to a reasonable extent in the 550−750 nm region, suggesting possibility of Förster-type energy transfer from MEH−PPV to PHT.[10c]

Figure 5a shows the absorption spectra of thin films of PHT/MEH−PPV binary blends. The absorption band of PHT clearly shows up as a lower energy shoulder (610 nm) in the absorption spectra of the blends. The absorption spectra of the binary blends are in fact simple superposition of the absorption spectra of the homopolymers. New absorption features were not observed in the wavelength range of 300−800 nm, suggesting that the two blend components have no observable interaction in the ground states.

The thin film PL emission spectra of PHT/MEH−PPV blends are shown in Figure 5b. The same PL emission spectra, when normalized with respect to the MEH−PPV emission peak at 602 nm are shown in Figure 5c. It can be seen that the emission spectra of the blends are composed of contributions from both MEH−PPV and PHT. As the PHT concentration in the blends increased the intensities of the 660 and 720 nm bands in the blend PL emission spectra increased relative to the MEH−PPV emission band at 602 nm. The inset of Figure 5b shows the relative PL quantum efficiency of PHT/MEH−PPV blend thin films calculated by normalizing the integrated PL intensity with respect to MEH−PPV. The absorbance at the excitation wavelength (509 nm) was the same for all the blend films. The relative PL

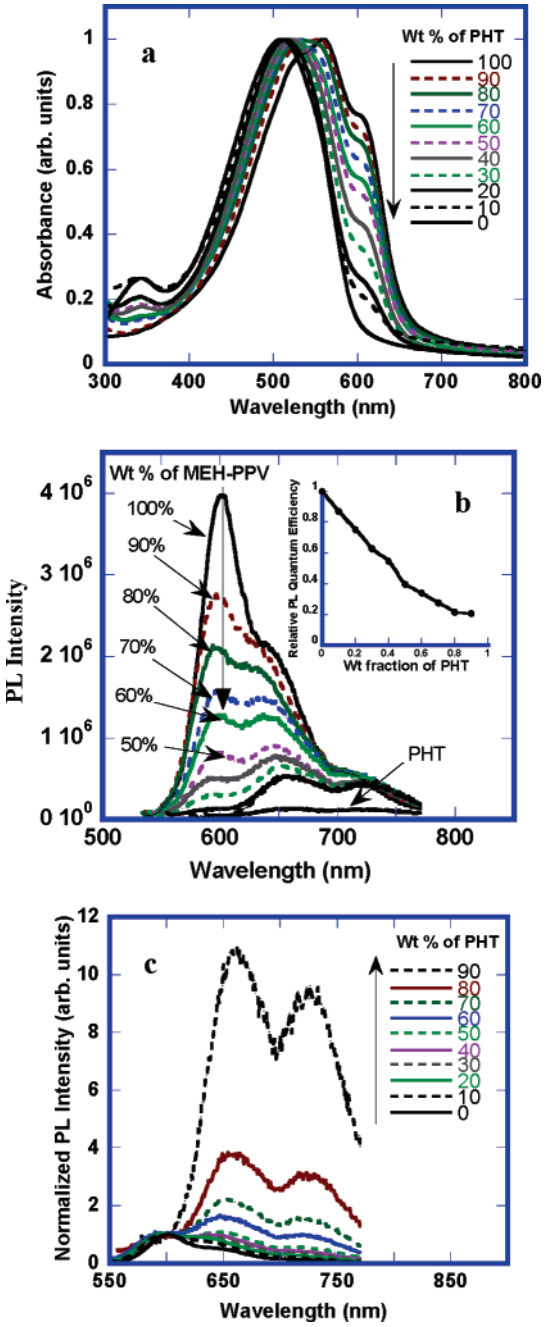

Figure 5. UV−vis absorption (a) and PL emission spectra (b, c) of PHT/MEH−PPV blends. Normalized PL emission with respect to MEH−PPV emission peak at 602 nm is shown in (c). Inset in (b) shows relative PL quantum efficiency of PHT/MEH−PPV blends.

quantum efficiency of the 50 wt % blend, for example, decreased by 60% compared to that of the MEH−PPV homopolymer. The observed quenching of MEH−PPV emission and enhancement in the intensity of the PHT emission band (Figure 5c) in the blends suggests some energy transfer from MEH−PPV to PHT as was observed previously.[16]

Polymer Blend Thin Film Transistors. All polymer blend field-effect transistors showed typical p-channel output characteristics (plot of drain current I_d vs drain voltage V_d at different gate voltages V_g) with accumulation mode operation. The field-effect mobility of holes was calculated from the slope of the $I_d^{1/2}$ vs V_g plot.[19] The PHT FETs fabricated under similar conditions as used for the blend FETs gave the field-effect

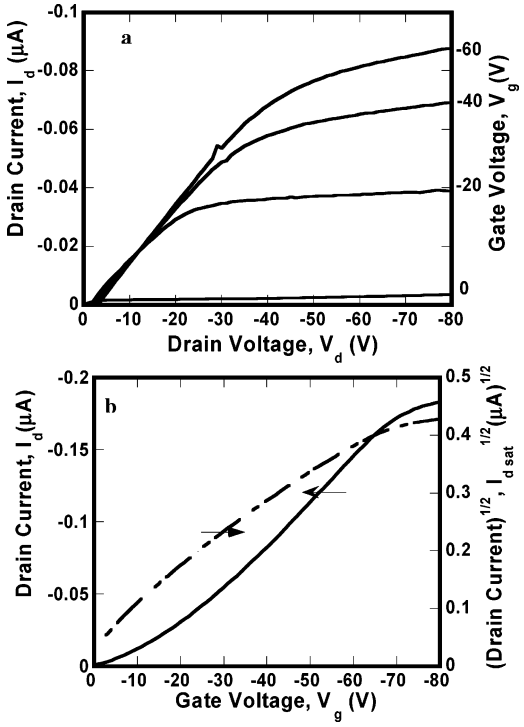

Figure 6. Output (a) and transfer characteristics (b) of a 60 wt % PHT/MEH−PPV blend FET.

mobility of holes in the 0.008−0.02 $cm^2/(V\ s)$ range with an I_{on}/I_{off} ratio of 10^4. To improve the off state characteristics, thermal annealing at 100 °C for 5 min was done, and this resulted in increase of the I_{on}/I_{off} ratio by at least 2 orders of magnitude. These results are in close agreement with the reported mobility of PHT devices fabricated under similar conditions.[4a,13b] The field-effect mobility of holes in MEH−PPV was measured to be 2×10^{-6} $cm^2/(V\ s)$, which is in close agreement with an earlier reported hole mobility ($(0.5-2.5) \times 10^{-6}$ $cm^2/(V\ s)$) determined by the time-of-flight method.[15c] However, a recent experimental and numerical analysis of MEH−PPV FETs gave a field-effect mobility of holes to be $(5-8) \times 10^{-5}$ $cm^2/(V\ s)$.[15d]

The PHT/MEH−PPV blend FETs were stable in air under the reduced light conditions used to determine the hole mobility. Representative FET output and transfer characteristics are shown in Figure 6 for a 60 wt % PHT blend. The field-effect mobility calculated from the saturation region of the 60 wt % PHT blend was 3×10^{-4} $cm^2/(V\ s)$ with a corresponding I_{on}/I_{off} ratio of 200. Similar FET results for the 80 wt % blend were 5×10^{-4} $cm^2/(V\ s)$ and 50. For the 40 wt % blend, the hole mobility was 2×10^{-4} $cm^2/(V\ s)$ with I_{on}/I_{off} ratio of 80. Thin-film transistors based on PHT/polystyrene blends also showed typical p-channel FET behavior. Representative output and transfer characteristics of this series of blends are shown in Figure 7 for a 50 wt % blend FET. The field-effect mobility of holes, calculated from saturation region, was 7×10^{-4} $cm^2/(V\ s)$ with an I_{on}/I_{off} ratio of 2×10^3. Similar results for the 20 wt % PHT blend were 3×10^{-5} $cm^2/(V\ s)$ and 2×10^3. In the case of the 80 wt % PHT blend, the hole mobility and on/off ratio were 4×10^{-3} $cm^2/(V\ s)$ and 30, respectively.

The compositional dependence of the field-effect mobility of holes in the PHT/MEH−PPV blend system is shown in Figure 8. Compared to the hole mobility in pure MEH−PPV, there is about 2 orders of magnitude

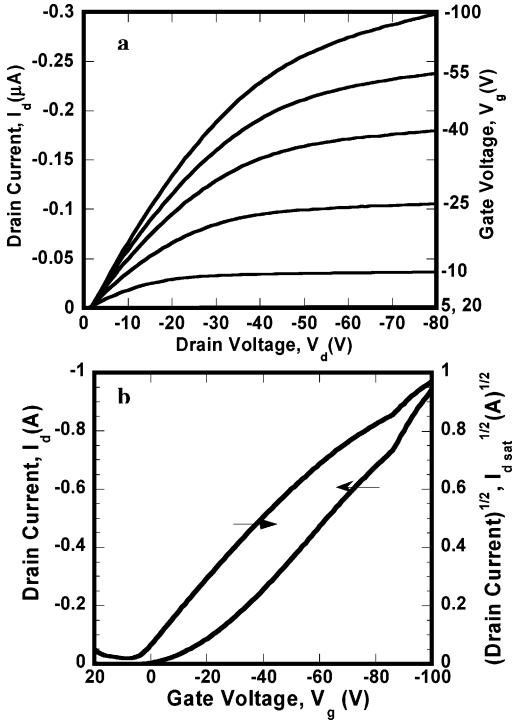

Figure 7. Output (a) and transfer characteristics (b) of a 50 wt % PHT/polystyrene blend FET.

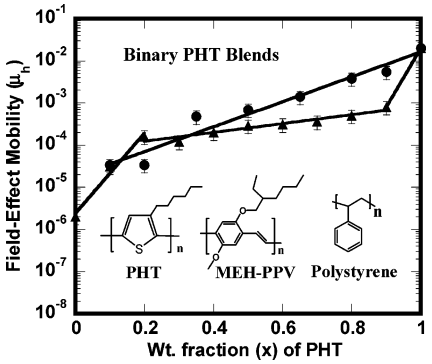

Figure 8. Compositional dependence of the field-effect mobility of holes in PHT/MEH−PPV blends (solid triangles) and PHT/polystyrene blends (solid circles).

increase in the hole mobility with only 20 wt % PHT present in the matrix of MEH−PPV. This represents a substantial increase in mobility; thus, 20 wt % PHT can be considered as a critical threshold concentration of PHT in the MEH−PPV matrix to achieve moderately high charge carrier mobility in the blends. Above 20 wt % PHT, the hole mobility has a weak exponential dependence on blend composition in the range $0.2 \leq x \leq 0.9$.[20] Compared to the mobility of holes in the pure PHT, there is a factor of about 20−25 decrease in carrier mobility when only 10 wt % of MEH−PPV is present in the blend. This substantial reduction in hole mobility when essentially an impurity amount of MEH−PPV (10 wt %) is present in PHT could not be due to MEH−PPV acting as a chemical trap for holes since the ionization potentials (HOMO levels) of PHT (IP = 4.7−5.1 eV)[21a,b] is lower or the same as MEH−PPV (IP = 5.1 eV). [21c] As further discussed below in comparison to the mobility of holes in PHT/polystyrene blends, a large part of the reduction in mobility can be traced to dipolar effects arising from the existence of permanent dipole moments in both PHT and MEH−PPV.

The compositional dependence of the field-effect mobility of holes in the PHT/polystyrene blend system is also shown in Figure 8. The dependence of the field-effect mobility of holes μ_h on the blend composition (x, weight fraction of PHT) is well described by an exponential, $\mu_h(x) = 1.8 \times 10^{-5} \exp(6.8x)$, over the entire composition range $0.1 \leq x \leq 1$. Since polystyrene is an insulator, the strong concentration dependence of the carrier mobility in the PHT/polystyrene blend system is reminiscent of features commonly observed in "molecularly doped" polymer systems.[17a−f] The energetic/positional disorder model of hopping transport that has provided a theoretical understanding of such molecularly doped insulating polymers[17] can also account for the charge transport in PHT/polystyrene blends. As the concentration of PHT within the polystyrene matrix decreases, the intersite distance between PHT chains or segments increases, which in turn reduces the carrier hopping rate. Below a critical concentration of PHT, the percolation threshold, the carrier hopping rate vanishes because of the rather large intersite distance. The observed threshold concentration is 10 wt % PHT in the PHT/polystyrene blend system.

A very surprising result is the finding from Figure 8 that the field-effect mobility of holes in PHT/polystyrene blends is larger than in PHT/MEH−PPV blends over almost the entire composition range. For example, at 90 wt % PHT the hole mobility is 5.5×10^{-3} cm^2/(V s) in PHT/polystyrene and 8×10^{-4} cm^2/(V s) in PHT/MEH−PPV. This is a factor of 7 higher mobility in the polystyrene blend compared to that of the MEH−PPV blend. Among the reasons why this result is surprising is that MEH−PPV is a p-type semiconductor with a very similar ionization potential to that of PHT whereas polystyrene is an insulator. Furthermore, both of the PHT blend systems have similar phase-separated morphologies as revealed by AFM and discussed previously. The reduced carrier mobility in the PHT/MEH−PPV blends compared to that in PHT/polystyrene blends can be understood as a consequence of dipolar effects, which are well-known phenomena in the molecularly doped polymer literature.[17] For example, the hole mobility of 1,1-bis(di-4-tolylaminophenyl)cyclohexane (TAPC)/polystyrene blends is known to be about 2 orders of magnitude higher than that in TAPC/bisphenol A−polycarbonate (PC) blends.[17c] The energetic- and positional-disorder hopping transport theory has successfully accounted for this, and similar experimental results in terms of the broadening of the width of the hopping site energy and position distributions when permanent dipole moments are present in the charge transport molecule (e.g., TAPC) and polymer host (e.g., PC).[17] In going from polystyrene with negligible dipole moment ($p = 0.1$ D) to the PC host ($p = 1.0$ D) for TAPC ($p = 1.0$ D), there is a significant broadening of the density of states and increase in the positional disorder, leading to random local fields that localize carriers and substantially reduce the carrier mobility. The high polarity of the present PHT ($p \sim 5.5$ D)/MEH−PPV ($p \sim 3.15$ D) blend components means that the observed reduction in hole mobility can be readily explained by such dipolar effects.

In all the polymer blend systems that we have studied so far, PHT/poly(3-decylthiophene) (PDT, IP = 5.0−5.2 eV),[13b] PHT/ poly(9,9-dioctylfluorene) (PFO, IP = 5.8 eV),[13c] and PHT/MEH−PPV, PHT/polystyrene (IP > 6.0 eV), the IP of PHT is either lower than or the same as

that of the other blend component so that the holes cannot be trapped in the low-mobility blend components. The hole mobilities of previously reported PHT/PDT ($p \sim 7.25$ D) ($0.6 \leq x \leq 1$) and PHT/PFO ($p \sim 1.73$ D) ($0.3 \leq x \leq 1$) blend systems were also lower than those of the present PHT/polystyrene blends. Our recently observed ambipolar charge transport in binary blends of poly(benzobisimidazobenzophenanthroline) (BBL) and copper phthalocyanine (CuPc)[13d] can now also been understood as evidence of dipolar effects on the field-effect mobility of charge carriers. In that BBL/CuPc blend system, the HOMO/LUMO energy levels for BBL (5.9 eV/4.0 eV) and CuPc (5.1 eV/3.5 eV) were such that CuPc cannot trap electrons and BBL cannot trap holes. Yet the ambipolar carrier mobilities were orders of magnitude lower than the respective unipolar mobilities of the components. We conclude that our present and previous results of studies of charge transport in blends of conjugated polymers demonstrate that dipolar effects significantly reduce carrier mobilities in blends of polymer semiconductors.

Conclusions

Binary PHT/MEH−PPV and PHT/polystyrene blends were found to be phase-separated on the length scale of 100−150 and 400−600 nm, respectively. AFM characterization showed that the morphology of the phase-separated PHT/MEH−PPV and PHT/polystyrene blends was of the nucleation and growth type when one of the blend components was present in the minority. In the case of the PHT/MEH−PPV blends, the morphology changes to an interpenetrating bicontinuous network as a result of spinodal decomposition around the symmetric composition (50 wt % PHT). Two orders of magnitude higher field-effect mobility ($(2-8) \times 10^{-4}$ cm^2/(V s)) in PHT/MEH−PPV blends was observed compared to that in the MEH−PPV homopolymer (2×10^{-6} cm^2/(V s)). The hole mobility of PHT/polystyrene blends was up to a factor of 7 higher than that of PHT/MEH−PPV blends and showed an exponential dependence on blend composition. The observed reduction of hole mobility in PHT/MEH−PPV blends relative to the PHT/polystyrene blend system was explained in terms of dipolar effects which arise from the existence of large permanent dipole moments in both conjugated polymer components. Because conjugated polymers are highly polar molecules, such dipolar effects are expected to play a critical role in modifying the charge carrier mobilities of their blends.

Acknowledgment. This research was supported by the Air Force Office of Scientific Research (Grant F49620-03-1-0162) and in part by the Boeing-Martin Professorship Endowment.

References and Notes

(1) (a) Heeger, A. J. *Angew. Chem., Int. Ed.* **2001**, *40*, 2591. (b) MacDiarmid, A. G. *Angew. Chem., Int. Ed.* **2001**, *40*, 2581.
(2) (a) Kraft, A.; Grimsdale, A. C.; Holmes, A. B. *Angew. Chem., Int. Ed.* **1998**, *37*, 402. (b) Bernius, M. T.; Inbasekaran, M.; O'Brien, J.; Wu, W. *Adv. Mater.* **2000**, *12*, 1737.
(3) (a) Sokolik, I.; Yang, Z.; Karasz, F. E.; Morton, D. C. *J. Appl. Phys.* **1993**, *74*, 3584. (b) Peng, Z.; Bao, Z.; Galvin, M. E. *Chem. Mater.* **1998**, *10*, 2086. (c) Jenekhe, S. A.; Zhang, X.; Chen, X. L.; Choong, V.-E.; Gao, Y.; Hsieh, B. R. *Chem. Mater.* **1997**, *9*, 409. (d) Tarkka, R. M.; Zhang, X.; Jenekhe, S. A. *J. Am. Chem. Soc.* **1996**, *118*, 9438. (e) Zhang, X.; Jenekhe, S. A. *Macromolecules* **2000**, *33*, 2069. (f) Alam, M. M.; Jenekhe, S. A. *Chem. Mater.* **2002**, *14*, 4775.
(4) (a) Bao, Z.; Dodabalapur, A.; Lovinger, A. J. *Appl. Phys. Lett.* **1996**, *69*, 4108. (b) Sirringhaus, H.; Tessler, N.; Friend, R. H. *Science* **1998**, *280*, 1741.
(5) (a) Babel, A.; Jenekhe, S. A. *Adv. Mater.* **2002**, *14*, 371. (b) Babel, A.; Jenekhe, S. A. *J. Am. Chem. Soc.* **2003**, *125*, 13656.
(6) (a) Yu, G.; Gao, J.; Hummelen, J. C.; Wudl, F.; Hegger, A. J. *Science* **1995**, *270*, 1789. (b) Antoniadis, H.; Hsieh, B. R.; Abkowitz, M. A.; Jenekhe, S. A.; Stolka, M. *Synth. Met.* **1994**, *62*, 265. (c) Jenekhe, S. A.; Yi, S. *Appl. Phys. Lett.* **2000**, *77*, 2635. (d) Yu, G.; Heeger, A. J. *J. Appl. Phys.* **1995**, *78*, 4510.
(7) (a) Aubert, P.-H.; Argun, A. A.; Cirpan, A.; Tanner, D. B.; Reynolds, J. R. *Chem. Mater.* **2004**, *16*, 2386. (b) Fungo, F.; Jenekhe, S. A.; Bard, A. J. *Chem. Mater.* **2003**, *15*, 1264.
(8) (a) Sariciftci, N. S.; Smilowitz, L.; Heeger, A. J.; Wudl, F. *Science* **1992**, *258*, 1474. (b) Arias, A. C.; MacKenzie, J. D.; Stevenson, R.; Halls, J. J. M.; Inbasekaran, M.; Woo, E. P.; Richards, D.; Friend, R. H. *Macromolecules* **2001**, *34*, 6005. (c) Jenekhe, S. A.; de Paor, L. R.; Chen, X. L.; Tarkka, R. M. *Chem. Mater.* **1996**, *8*, 2401.
(9) (a) Jenekhe, S. A.; Osaheni, J. A. *Science* **1994**, *265*, 765. (b) Osaheni, J. A.; Jenekhe, S. A. *Macromolecules* **1994**, *27*, 739.
(10) (a) Berggren, M.; Inganas, O.; Gustafsson, G.; Rasmusson, J.; Andersson, M. R.; Hjertberg, T.; Wennerstrom, O. *Nature (London)* **1994**, *372*, 444. (b) Lee, J.-I.; Kang, I.-N.; Hwang, D.-H.; Shim, H.-K. *Chem. Mater.* **1996**, *8*, 1925. (c) Alam, M. M.; Tonzola, C. J.; Jenekhe, S. A. *Macromolecules* **2003**, *36*, 6577.
(11) (a) Zhang, X.; Kale, D. M.; Jenekhe, S. A. *Macromolecules* **2002**, *35*, 382. (b) Chen, X. L.; Jenekhe, S. A. *Appl. Phys. Lett.* **1997**, *70*, 487.
(12) Chen, X. L.; Jenekhe, S. A. *Macromolecules* **1997**, *30*, 1728.
(13) (a) Babel, A.; Jenekhe, S. A. *J. Phys. Chem. B* **2002**, *106*, 6129. (b) Babel, A.; Jenekhe, S. A. *J. Phys. Chem. B* **2003**, *107*, 1749. (c) Babel, A.; Jenekhe, S. A. *Macromolecules* **2003**, *36*, 7759. (d) Babel, A.; Wind, J. D.; Jenekhe, S. A. *Adv. Funct. Mater.* **2004**, *14*, 891.
(14) (a) Scherf, U.; Riechel, S.; Lemmer, U.; Mahrt, R. F. *Curr. Opin. Solid State Mater. Sci.* **2001**, *5*, 143. (b) Hide, F.; Diaz-Garcia, M. A.; Schwartz, B. J.; Andersson. M. R.; Pei, Q.; Heeger, A. J. *Science* **1996**, *273*, 1833.
(15) (a) Inigo, A. R.; Tan, C. H.; Fann, W.; Huang, Y.-S.; Perng, G.-Y.; Chen, S.-A. *Adv. Mater.* **2001**, *13*, 504. (b) Tan, C. H.; Inigo, A. R.; Fann, W.; Wei, P.-K.; Perng, G.-Y.; Chen, S.-A. *Org. Electr.* **2002**, *3*, 81. (c) Campbell, I. H.; Smith. D. L.; Neef, C. J.; Ferraris, J. P. *Appl. Phys. Lett.* **1999**, *74*, 2809. (d) Roichman, Y.; Tessler, N. *Appl. Phys. Lett.* **2002**, *80*, 151.
(16) Yu, G.; Nishino, H.; Heeger, A. J.; Chen, T.-A.; Rieke, R. D. *Synth. Met.* **1995**, *72*, 249.
(17) (a) Borsenberger, P. M.; Weis, D. S. *Organic Photoreceptors for Imaging Systems;* Marcel Dekker: New York, 1993. (b) Van der Auweraer, M.; De Schryver, F. C.; Borsenberger, P. M.; Bassler, H. *Adv. Mater.* **1994**, *6*, 199. (c) Borsenberger, P. M.; Bässler, H. *J. Chem. Phys.* **1991**, *95*, 5327. (d) Ries, B.; Bassler, H.; Silver, M. *Philos. Mag. B* **1986**, *54*, 141. (e) Goonesekera, A.; Ducharme, S. *J. Appl. Phys.* **1999**, *85*, 6506. (f) Sworakowski, J. *Braz. J. Phys.* **1999**, *29*, 318. (g) Hertel, D.; Bässler, H.; Scherf, U.; Hörhold, H. H. *J. Chem. Phys.* **1999**, *110*, 9214.
(18) Kulkarni, A. P.; Kong, X.; Jenekhe, S. A. *J. Phys. Chem. B* **2004**, *108*, 8689.
(19) (a) Sze, S. M. *Physics of Semiconducting Devices*; Wiley: New York, 1981. (b) Horowitz, G. *Adv. Mater.* **1998**, *10*, 365. (c) In the saturation regime ($V_d > V_g - V_t$, where V_t is the threshold voltage), I_d can be described using the equation $I_d = (W/2L)C_0\mu(V_g - V_t)^2$, where μ is the field-effect mobility, W is the channel width, L is the channel length, and C_0 is the capacitance per unit area of the gate dielectric layer (SiO_2, 300 nm, $C_0 = 11$ nF/cm^2).
(20) The hole mobility for most of the blend composition (20−90 wt % PHT) was found to be well described by an exponential expression: $\mu_h = 7.7 \times 10^{-5} \exp(2.4x)$, with $R = 0.97$.
(21) (a) Johansson, T.; Mammo, W.; Svensson, M.; Andersson, M. R.; Inganäs, O. *J. Mater. Chem.* **2003**, *13*, 1316. (b) Nakanishi, N.; Tada, K.; Onoda, M.; Nakayama, H. *Appl. Phys. Lett.* **1999**, *75*, 226. (c) Li, Y.; Cao, Y.; Gao, J.; Wang, D.; Yu, G.; Heeger, A. J. *Synth. Met.* **1999**, *99*, 243.

MA0482314